DOI: 10.1109/TASC.2022.3147137
FERMILAB-PUB-22-257-TD (accepted)

Magnetic, Mechanical and Thermal Modeling of Superconducting, Whole-body, Actively Shielded, 3 T MRI Magnets Wound Using MgB_2 Strands for Liquid Cryogen Free Operation

M. Majoros, M. D. Sumption, M. Parizh, F. Wan, M. A. Rindfleisch, D. Doll, M. Tomsic, and E. W. Collings

***Abstract*—we present magnetic, mechanical and thermal modeling results for a 3 Tesla actively shielded whole body MRI (Magnetic Resonance Imaging) magnet consisting of coils with a square cross section of their windings. The magnet design was a segmented coil type optimized to minimize conductor length while hitting the standard field quality and DSV (Diameter of Spherical Volume) specifications as well as a standard, compact size 3 T system. It had an overall magnet length and conductor length which can lead to conduction cooled designs comparable to NbTi helium bath cooled 3 T MRI magnets. The design had a magnetic field homogeneity better than 10 ppm (part-per-million) within a DSV (Diameter of Spherical Volume) of 48 cm and the total magnet winding length of 1.37 m. A new class of MgB_2 strand especially designed for MRI applications was considered as a possible candidate for winding such magnets. This work represents the first magnetic, mechanical and thermal design for a whole-body 3 T MgB_2 short (1.37 m length) MRI magnet based on the performance parameters of existing MgB_2 wire. 3 Tesla MRI magnet can operate at 20 K at 67 % of its critical current.**

***Index Terms*—Magnetic Resonance Imaging, Superconducting magnet, conduction cooling.**

I. Introduction

MAGNETIC resonance imaging (MRI) is an important technique for medical diagnosis [1] because it provides good soft tissue contrast without using ionizing radiation. Practical MRI magnet designs require actively shielded magnets [2] – [4] for a number of reasons including ease of sitting. At the present time most of the superconducting MRI magnets use low temperature superconductors (e.g. NbTi, critical temperature T_c = 9 K) operating in liquid He bath at 4.2 K or below. With the rising cost and limited supply of helium, liquid cryogen free MRI development has become of strong interest for the MRI industry. Conduction cooled systems are also of interest because of a greater potential for magnet design flexibility, with benefits to functionality and patient comfort. Efforts to develop conduction cooled MRIs have followed two tracks. In the first track, the focus has been on better engineering designs for the conduction cooling system as well as other design aspects so that NbTi can still be used. While in principle this can be done, such designs have natural limitations because of the low minimum quench energy (MQE) of NbTi strand. This puts pressure on these designs to use low operational current (I_{op}) to critical current (I_c) ratios (which leads to a need for more conductor) and other design complications to mitigate the potential for quenching in a dry system. The second route has been to consider higher T_c conductors, where both more temperature margin is present, and the MQE is much larger. However, MRIs are commercial, and cost is a driver, so any potential replacement system must meet the same cost goals as the NbTi systems they might replace.

A recent paper [5] has considered a variety of superconductors beyond NbTi for 1.5 T whole body MRIs, and we can expect the analysis to be quite similar for 3 T machines, except for of course even higher performance requirements. HTSC conductors including YBCO and Bi2212 or Bi2223 were found to have significant cost problems as well as either undesirable strand aspect ratios (YBCO and Bi2223) or undesirable reaction heat treatment schedules (Bi:2212). In addition, these conductors at present lack practical superconducting jointing technology. Given the above limitations and the additional cost of actively driven systems, HTSC for commercial 1.5 or 3 T systems seems unlikely. For MgB_2, the analysis of Ref [5] showed that of all presently available conductors, in-situ route MgB_2 was the conductor beyond NbTi most ready for MRI applications. The main issues that were called out for practical MgB_2 MRIs were the need for commercially available long lengths of low cost conductor, the improvement of the joining technology, and development of MRI-specific conductor designs.

Recent publications from our collaboration with Hyper Tech Research company and Case Western Reserve University have shown the development of MRI-specific MgB_2 designs [4], [6], the demonstration of an MgB_2 superconducting

(Style: TAS First page footnote) Manuscript receipt and acceptance dates will be inserted here. Acknowledgment of support is placed in this paragraph as well. Consult the IEEE *Editorial Style Manual* for examples. This work was supported by the IEEE Council on Superconductivity under contract. ABCD-123456789.
(Corresponding author: M. Majoros)
M. Majoros, M. D. Sumption, E. W. Collings are with the Ohio State University, Columbus, OH 43210, USA.
M. Parizh is with General Electric Global Reseach, Niskayuna, NY, USA.
F. Wan is with FermiLab, Batavia, IL, USA
M. A. Rindfleisch, D. Doll, M. Tomsic are with Hyper Tech Research, Inc., Columbus, OH, USA.
Color versions of one or more of the figures in this paper are available online at http://ieeexplore.ieee.org.
Digital Object Identifier will be inserted here upon acceptance.

joint, and the fabrication and test of a sub-size react and wind MgB_2 MRI coil segment [7] – [9]. However, a 3 T MRI design which has the potential to be commercially viable is also needed. Several useful designs of 1.5 and 3 T systems based on MgB_2 have been published [3,4], but the amount of conductor and magnet length were larger than desired.

This work demonstrates a 3 T MRI with a magnet length and conductor length comparable to that of existing NbTi systems, and thus points to the potential for commercially viable designs.

II. Electromagnetic Modeling

A geometry with the |B| field map of the 3 T MRI magnet is shown in Fig.1. To achieve 3 T on-axis field the magnet needs a winding engineering current density of 94.251 A/mm^2. Maximum field on the end turns reaches a value of 6.54 T. Magnet winding length = 1.367 m, volume of superconductor = 0.26158 m^3, coil weight = 1625.72 kg, minimum inner winding radius (positioned in the ends of the winding) is 0.4375 m, maximum inner winding radius (positioned in the central part of the magnet) is 0.4714 m, outer winding radius is 0.9447 m.

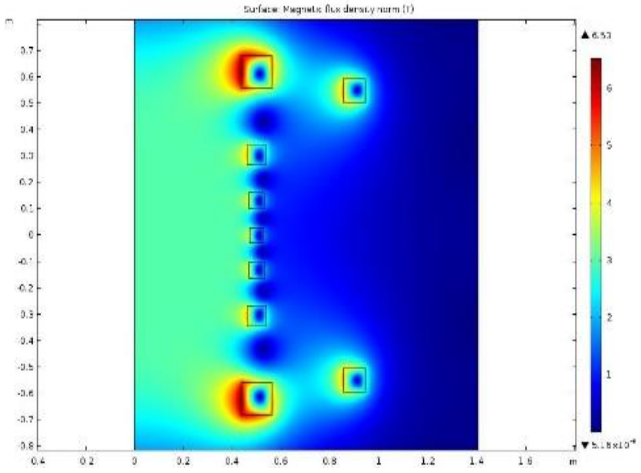

(a)

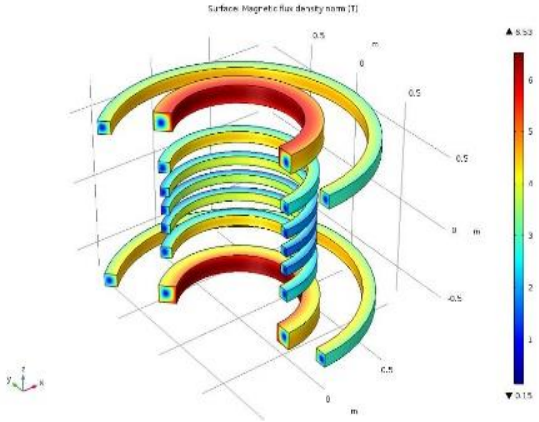

(b)

Fig. 1. |B| map at winding engineering current density of 94.251 A/mm^2 (max. on-axis field = 3T, max. field in the winding = 6.54 T. (a) 2D view, (b) 3D view.

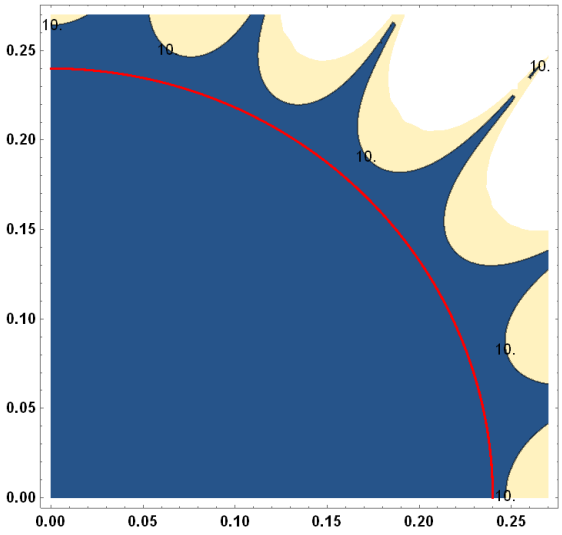

Fig. 2. 10 ppm homogeneity in DSV = 0.5 m (2D view, only a quarter of geometry shown, *x*-coordinate in axial direction, *y*-coordinate in radial direction)

Fig. 2 shows the homogeneity of the magnetic field in the magnet central part (10ppm is achieved in DSV of 0.5 m). 4.2 K I_c and n-value of an MgB_2 18-filamentary advanced-internal magnesium-infiltration (AIMI) strand (0.84 mm OD) [6] is shown in Fig. 3.

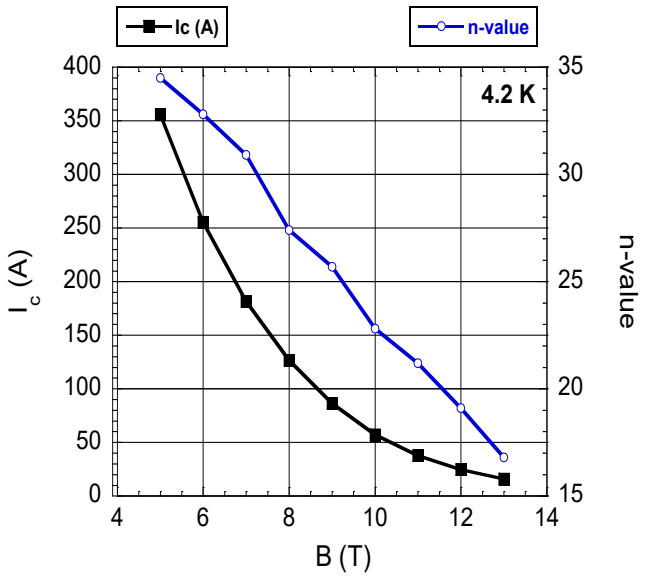

Fig. 3. 4.2 K critical current and n-value of 2G MgB_2 strand (0.84 mm OD) used in the modeling.

For achieving 3 T on-axis field the magnet needs the winding engineering current density of 94.251 A/mm^2. At 6.54 T the critical current of our 2G MgB_2 wire (0.84 mm OD) is approximately 200 A (Fig. 3). Translated to the engineering critical current density of the wire we get $J_{c\ engn\ wire}$ (6.54T,4.2K) = 360.895 A/mm^2. At a temperature of 20 K we then have $J_{c\ engn\ wire}$ (6.54T,20K) = 187.0495 A/mm^2. This value translated to the engineering critical current density of the winding (and considering a fill factor of the winding 0.75, which assumes a rectangular wire geometry 1.19 mm x 1.81 mm with insulation) gives the

value $J_{c\ engn\ winding}$ (6.54T,20K) = 140.287 A/mm^2. This means that at the temperature of 20 K the MRI magnet can achieve 3 T on-axis field at the current 67% of its critical current, which is a quite acceptable value from the view point of stability as well as from the point of view of persistent operation (the averaged magnetic field decay should not exceed 0.1 ppm/hour [10]).

III. Mechanical Modeling

Our choice of construction materials of the magnet was affected by the possibility of its conduction cooling. This calls for materials with good thermal conductivity and with sufficiently high yield strength at the same time. Operational temperature of our MRI magnet will be 4 K – 20 K. For outside cryogenic jacket of the magnet we intend to use a stainless steel. Ferric, martensitic and duplex stainless steels tend to become brittle as the temperature is reduced, in a similar way to other ferritic / martensitic steels. The austenitic stainless steels such as 304 and 316 are however 'tough' at cryogenic temperatures and can be classed a 'cryogenic steels'. This is the result of the 'fcc' (face centered cube) atomic structure of the austenite, which is the result of the nickel addition to these steels. We have chosen 316 steel because it has a higher resistance to corrosion. So the cryostat can better perform if moved in a humid environment.

The former of the winding as well as its bandage is assumed to be made of cold worked copper (26% cold work)[11]. Thermal conductivity of copper is weakly affected by cold work [3]. At 26% cold work the thermal conductivity of copper decreases only by about 5% [12]. Mechanical properties of the superconducting winding were considered based on the analysis given in [13]. The wire will be electrically insulated by fiber glass epoxy. We see that apart from epoxy, all the constituent materials (MgB_2, Nb, Monel [6]) have much higher moduli of elasticity – about 5-times higher than epoxy. Therefore, as a worst case scenario, we assumed that for our mechanical modeling purposes the superconducting winding has the mechanical parameters of the epoxy. Mechanical design of the magnet is schematically shown in Fig. 4.

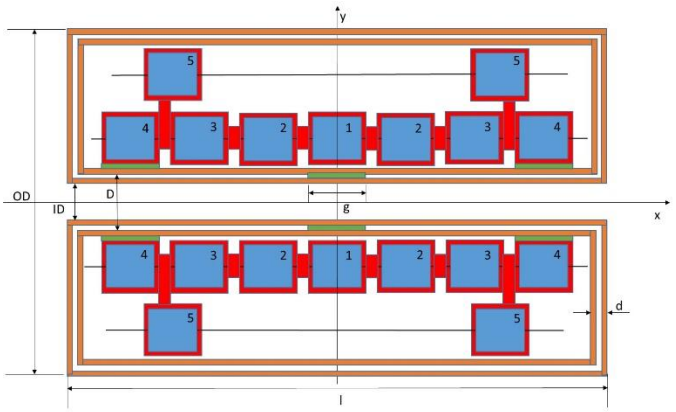

Fig. 4. Schematics of the mechanical design (x = axis of rotation). Blue – superconducting winding, red – copper former, brown – stainless steel cryostat (wall thickness = 1 cm), green – G10 fiber-glass epoxy mechanical support (1 cm thick). Magnet length including cryogenics l = 1.4715 m, cryostat OD = 1.9877 m, cryostat warm bore ID = 0.77 m, d = 3 cm, g = 15 cm.

Full geometry of the MRI magnet, including cryogenics, is shown in Fig. 5.

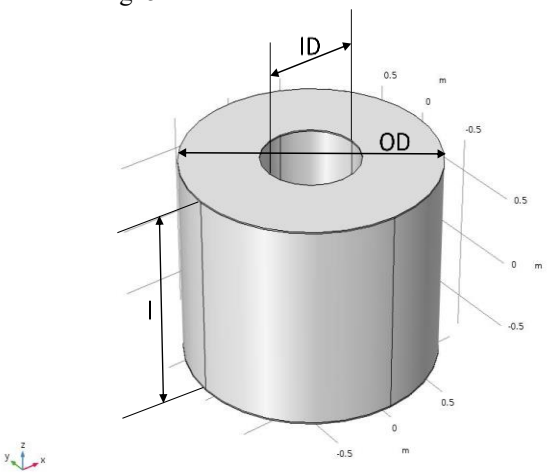

Fig. 5. Full geometry of the MRI magnet: Magnet length *l* = 1.4715 m, magnet OD = 1.9877 m, magnet ID = 0.77 m.

Electromagnetic forces obtained from the electromagnetic modeling were considered as mechanical loads in this modeling. Von Mises stress distribution in the whole magnet cross-section is shown in Fig. 6.

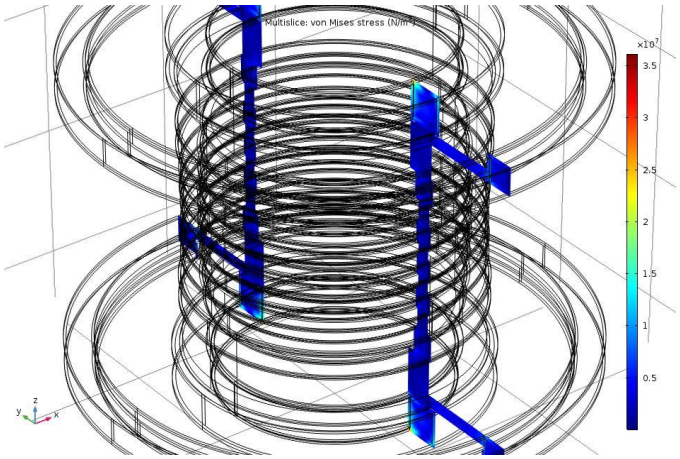

Fig. 6. Von Mises stress in Cu former and winding.

For react-and-wind MgB_2 wire an acceptable strain is < 0.4% (with no I_c degradation). From our mechanical modeling we obtained the strain value of 0.04 % which is one order of magnitude less than the wire strain tolerance. This means that no critical current degradation of the MgB_2 wire will occur. Our mechanical design provides a lower strain value (0.04%) than the design of 1.5 T MRI reported in [13] which gives the strain of 0.06%.

Maximum von Mises stress is located in Cu former (Fig. 6) – in its top and bottom parts and it represents 44.9% of the copper yield strength. All these results indicate that our MRI magnet will be mechanically stable.

IV. Thermal Modeling

In this model the outer surface of the inner SS cylinder (Fig. 4) is considered to be connected to the 1st stage of the cryocooler's cold head and simultaneously exposed to a thermal radiation coming from the outer SS cylinder (Fig. 4) supposed to be at ambient temperature. Cu formers of the MgB_2 winding are supposed to be connected to the 2nd stage of the cryocooler's cold head and simultaneously exposed to a thermal radiation coming from the inner SS cylinder connected to the 1st stage of the cryocooler's cold head. The cooling powers of the cryocoolers considered in this study are taken from Sumitomo company data [14]. Both, the inner SS cylinder as well as the coils are supposed to be wrapped in a superinsulation foil (aluminized Mylar) to suppress the thermal radiation effects. With N "floating" (not thermally anchored) metallic radiation shields, the radiative heat transfer is reduced by a multiplicative factor of about 1/(N+1) [15]. For best results, the layer density typically should be about 30 layers/cm [15]. In our FEM modeling we used 30 layers of Mylar (occupying 1 cm). Considering a common condition of polished surfaces of SS and Cu (with emissivity ε= 0.02) for 30 layers of Mylar we get ε= 6.45e-4. Thermal properties of the materials used in modeling have been obtained from literature sources as well as from the data base provided in the COMSOL software used for FEM modeling [4, 15, 16].

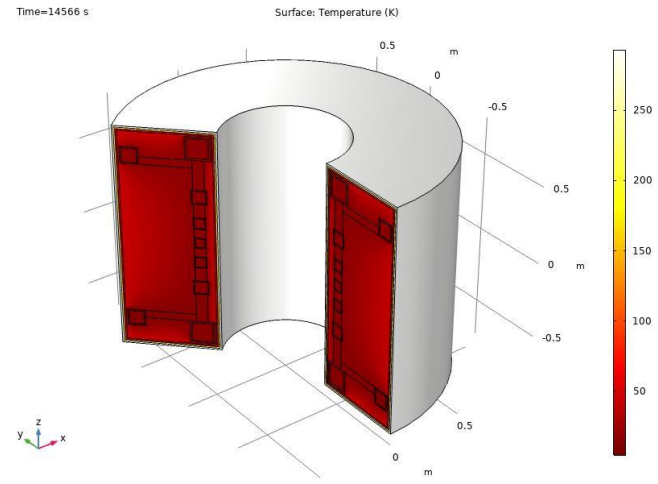

a)

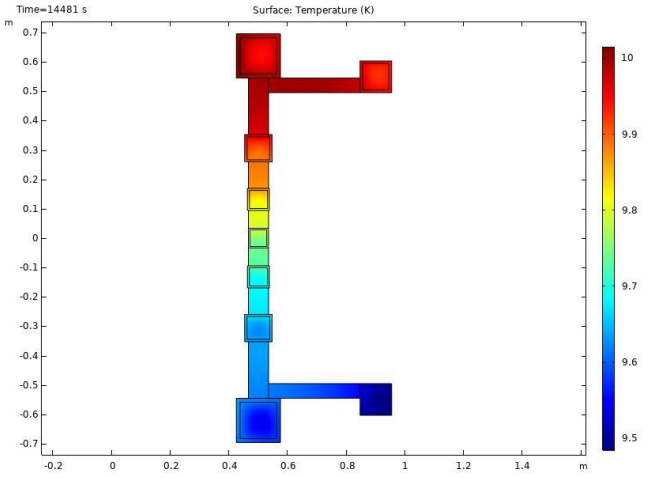

b)

Fig. 7. Temperature maps in the MRI winding around 10K. (a) 3D map, (b) 2D map.

For cooling down we considered 1 Sumitomo cryocooler – RDK-415D2 cold head with CSW-71D compressor. In the modeling we considered heat transfer via conduction as well as via surface-to-surface radiation. To suppress heat radiation a use of superinsulation was considered as mentioned above. For cooling we assumed the magnet was pre-cooled with liquid nitrogen to 77 K. Starting from this temperature one cryocooler was able to cool the magnet down to 10 K during 8.25 hours. Fig 7 shows the temperature distribution across the winding. At a level of 10 K the maximum temperature difference across the winding was 0.53 K which is acceptable. In this simple model we considered the cooling power of the cold head as a boundary condition with homogeneously distributed cooling power. Consideration of real dimensions and position of the cold head with cooling straps distributed throughout the magnet former and winding as well as with a heat leak from current leads will be a subject of a more complex modeling.

V. Conclusions

Using 2G MgB_2 wire (advanced-internal magnesium-infiltration) 3T MRI winding (1.367m long) can be realized. Former of the winding made of cold work Cu (26% cold work) provides a good mechanical support and at same time allows a good conduction cooling using just one Sumitomo cryocooler. For initial cool down, after the magnet was pre-cooled by liquid nitrogen, one Sumitomo cryocooler would need 8.25 hours to cool the magnet down to 10 K. Mechanical forces and thermal gradients are on an acceptable level. Because of higher T_c of MgB_2 material (about 37 K for wires), 3T MRI magnet can operate at 67% of its I_c (at 6.54 T) at 20 K, at the same weight of the conductor.

Acknowledgment

This work was supported by the National Institute of Biomedical Imaging and Bioengineering, National Institutes of Health (NIH), under Grant R01EB018363 and an NIH Bridge Grant.

References

[1] C. Cosmus, M. Parizh, "Advances in whole-body MRI magnets," *IEEE Trans. Appl. Supercond.,* vol. 21, 2011, 2104.

[2] Y. Lvovsky, E W Stautner, T. Zhang, "Novel technologies and configurations of superconducting magnets for MRI," *Supercond. Sci. Technol.,* vol. 26, 2013, 93001.

[3] T. Baig, Z. Yao, D. Doll, M. Tomsic, M. Martens, "Conduction cooled magnet design for 1.5 T, 3.0 T and 7.0 T MRI systems," *Supercond. Sci. Technol.* vol. 27, 2014, 125012.

[4] T. Baig, A. Amin, R. Deissler, L. Sabri, C. Poole, R. W. Brown, M. Tomsic, D. Doll, M. Rindfleisch, X. Peng, R. Mendris, O. Akkus, M. Sumption, M. Martens, "Conceptual designs of conduction cooled MgB_2 magnets for 1.5 T and 3.0 T full body MRI systems," *Supercond. Sci. Technol.* vol. 30, 2017, 043002.

[5] M. Parizh, Y. Lvovsky, M. Sumption, "Conductors for commercial MRI magnets beyond NbTi: requirements and challenges," *Supercond. Sci. Technol.* vol. 30, 2017, 014007.

[6] F. Wan, M. D. Sumption, M. A. Rindfleisch, M. J. Tomsic, C. J. Thong, E. W. Collings, 2020 "High performance, advanced - internal - magnesium - infiltration (AIMI) MgB_2 wires processed using a vapor-solid reaction route," *Supercond. Sci. Technol.* vol.33, 2020, 094004.

[7] H. S. Kim, C. Kovacs, M. Rindfleisch, J. Yue, D. Doll, M. Tomsic,M. D. Sumption, E. W. Collings, "Demonstration of a Conduction Cooled React and Wind MgB_2 Coil Segment for MRI Applications," *IEEE Trans. Appl. Supercond*. Vol. 26, 2016, 4400305.

[8] D. Zhang, C. Kovacs, J. Rochester, M. Majoros, F. Wan, M. D. Sumption, E. W. Collings, M. Rindfleisch, D. Panik, D. Doll, R. Avonce, M. Tomsic, C. Poole, L. Sabri, T. Baig, M. Martens, "Instrumentation, cooling, and initial testing of large, conduction-cooled, react-and-wind MgB_2 coil segment for MRI applications," *Supercond. Sci. Technol.* vol.31, 2018, 085013.

[9] D. Zhang, M. Sumption, M. Majoros, C. Kovacs, E. Collings, D. Panik, M. Rindfleish, D. Doll, M. Tomsic, C. Poole, M. Martens, "Quench, normal zone propagation velocity, and the development of an active protection scheme for a conduction cooled, react-and-wind, MgB_2 MRI coil segment," *Supercond. Sci. Technology* vol. 32, 2019, 125003.

[10] M. Parizh, W. Stautner "MRI Magnets," *Handbook of Superconducting Materials,* Taylor and Francis editors, 2020.

[11] R. P. Reed, R. P. Mikesell, "Low temperature mechanical properties of copper and selected copper alloys," National Bureau of Standards Monograph 101, Issued December 1, 1967.

[12] A. Williams, "Effect of cold work on the thermal conductivity of copper," *J. Mech. Engn. Sci.*, vol. 7, 1965, 335.

[13] A. A. Amin, T. Baig, R. J. Deissler, Z. Yao, M. Tomsic, D. Doll, O. Akkus, M. Martens, "A multiscale and multiphysics model of strain development in a 1.5 T MRI magnet designed with 36 filament composite MgB_2 superconducting wire," *Supercond. Sci. Technol.* vol. 29, 2016, 055008.

[14] http://www.shicryogenics.com/

[15] J. W. Ekin, "Experimental techniques for low-temperature measurements – cryostat design, material properties, and superconductor critical current testing," Oxford University Press, 2006.

[16] COMSOL Multiphysics https://www.comsol.com